MR evaluation of spinal dermal sinus tracts in children.

A J Barkovich, M s Edwards and P H Cogen

AJNR Am J Neuroradiol 1991, 12 (1) 123-129
http://www.ajnr.org/content/12/1/123

MR Evaluation of Spinal Dermal Sinus Tracts in Children

A. James Barkovich[1,2]
Michael S. B. Edwards[2]
Philip H. Cogen[2]

The MR studies of seven pediatric patients with surgically proved spinal dorsal dermal sinuses were reviewed retrospectively. Five of the seven had associated congenital tumors (three epidermoids, two dermoids). The subcutaneous portions of the spinal tracts and intramedullary portions of tumor were easily identified with the use of standard spin-echo techniques. However, except for limited areas where they were lined by fat, the intraspinal portions of the dermal sinuses were poorly seen. Moreover, diffuse subarachnoid tumor was missed in two patients. Three-dimensional Fourier transform gradient-echo acquisition using a volumetric radiofrequency pulse as a "spoiler" proved to be helpful in evaluating these abnormalities.

Optimal radiologic workup of patients with dorsal dermal sinuses awaits the development of new MR imaging sequences. For now, heavily T1-weighted MR sequences should be obtained and supplemented with sonography in infants and with CT myelography in older children.

***AJNR* 12:123–129, January/February 1991; *AJR* 156: April 1991**

The advent of MR imaging has greatly facilitated the diagnosis of developmental anomalies of the CNS, which are now easily and noninvasively diagnosed [1–3]. The improvement in imaging techniques has been especially valuable in the spine, where the shape and location of the spinal cord and the presence of associated fatty tumors are readily demonstrated [1, 4, 5].

We have recently had the opportunity to review the imaging studies of seven patients with surgically proved spinal dermal sinus tracts, five of whom had associated dermoid or epidermoid tumors. All were examined with standard spin-echo MR techniques. We found that, in contradistinction to most spinal anomalies, spinal dorsal dermal sinuses were difficult to assess adequately by using conventional spin-echo imaging techniques. The purpose of this article is to report the pathologic anatomy of these patients as detected by MR, to compare the MR findings with the surgical findings, to point out the potential pitfalls of MR in the workup of this anomaly, and to make suggestions for the most efficacious radiologic workup.

Materials and Methods

MR scans of seven patients with surgically proved dorsal dermal sinuses of the spine were reviewed retrospectively (Table 1). The average age of the five girls and two boys was 4 years old (range, 4 months to 11 years). Three patients were asymptomatic; the abnormalities were detected by the presence of a midline skin dimple at the lumbosacral level (one) or a focal skin dysplasia, cutis aplasia (two). Two patients presented with urinary bladder dysfunction and lower extremity spasticity; one of these patients had a dimple at the L5 level, the other at S1. Patient 6 presented because of persistent low back pain that worsened with flexion and extension. Patient 4 presented with an acute myelopathy and a C5 sensory level.

Six patients were studied at 1.5 T; the seventh was studied at 0.6 T. Sagittal 3-mm spin-

Received June 26, 1990; revision requested September 6, 1990; revision received September 27, 1990; accepted September 28, 1990.

[1] Department of Radiology, Box 0628, Neuroradiology Section, L371, University of California, San Francisco, CA 94143. Address reprint requests to A. J. Barkovich.

[2] Department of Neurological Surgery, University of California, San Francisco, CA 94143.

0195-6108/91/1201-0123

echo (SE) 600–1000/20/2 (TR/TE/excitations) images were obtained in patients 1, 3, 4, 5, and 6, using a 256 × 192 matrix. Sagittal 5-mm SE 1800/30, 80/2 images were obtained in patient 6, and sagittal 5-mm SE 533/28/2 images were obtained in patient 2. Axial 5-mm SE 600–1000/20/2 images were obtained in patients 1, 3, 4, 5, 6, and 7. No axial images were available for patient 2.

The MR studies were assessed for the presence and level of the cutaneous lesion, the presence of any bony spinal deformities, the

TABLE 1: Data for Seven Patients with Spinal Dermal Sinus

Patient No.	Age	Sex	Presenting Signs/Symptoms	Conus Level	Skin Defect Level	Character of Tract	Character of Tumor	
							Surgical	Radiologic
1	4 mo	M	Lumbar cutis aplasia	L3–L4	L4	Short T1, curvilinear L2–L5 adherent to right dorsal roots	N/A	N/A
2	6 mo	F	Thoracic cutis aplasia	T12–L1	T10	Intraspinal part not seen	Intra- and extramedullary dermoid at T8–T9	Intra- and extramedullary mass at T8–T9, isointense with CSF
3	18 mo	F	Sacral dimple	L4–L5	L5/S1	Lined by fat (short T1), tract itself not seen, curvilinear L3 to L4–L5	N/A	N/A
4	20 mo	F	Acute myelopathy, C5 sensory level	L1	T7	Intraspinal part not seen	Intramedullary dermoid at T3 to T5–T6	Intramedullary mass at T3 to T5–T6, isointense with CSF
5	3 yr	M	Lower extremity weakness and spasticity, neurogenic bladder	L3	L5	Intraspinal part not seen	Midlumbar extramedullary epidermoid	Midlumbar extramedullary epidermoid, circle of nerve roots surrounded mass, isointense with CSF
6	6 yr	F	Back pain, meningismus	T12–L1	L4–L5	Intraspinal part not seen	Ruptured intra- and extramedullary epidermoid from T12 to sacrum	Indistinct mass, slightly short T1
7	11 yr	F	Back pain	Mid L3	S1	Intraspinal part not seen	Ruptured extramedullary dermoid, conus to sacrum	Areas of short T1 and T2, most areas isointense with CSF

Note. — N/A = not applicable.

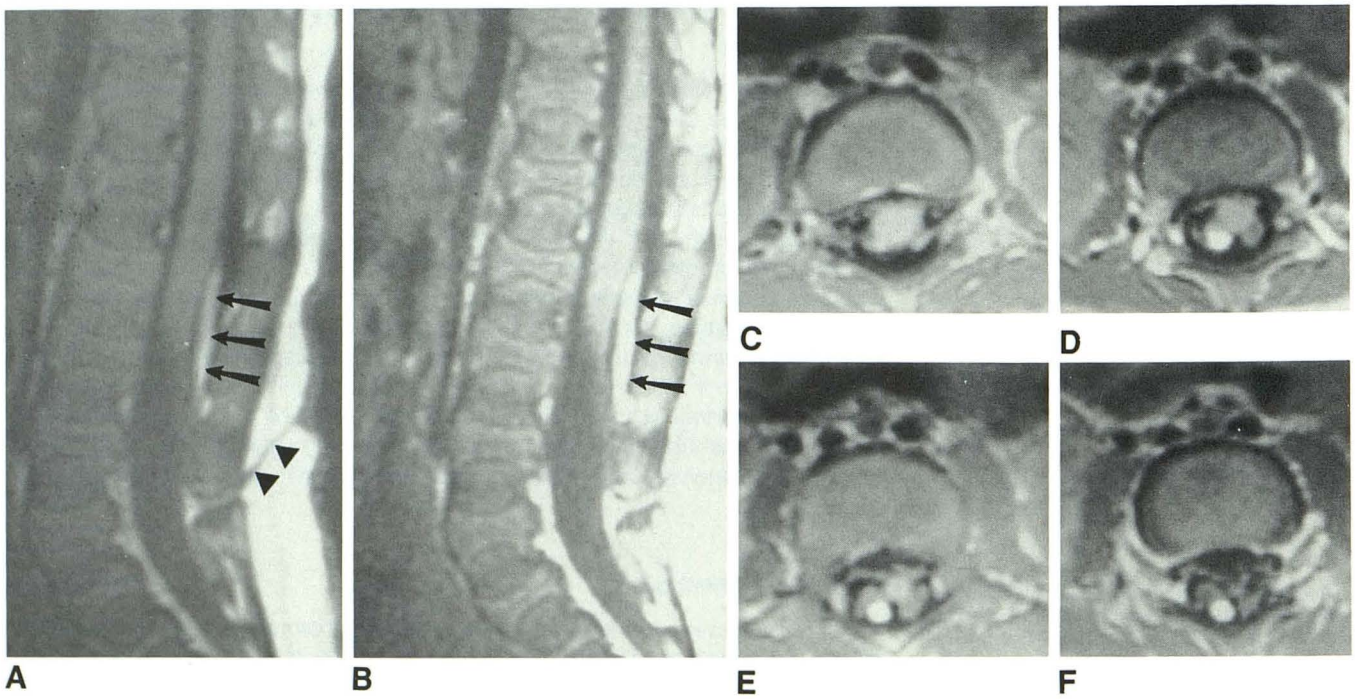

Fig. 1.—Patient 1.

***A* and *B*, Sagittal SE 600/20 images with wide windowing (*A*) and narrow windowing (*B*). Both images show tethering of cord, with conus at L3–L4 level and fat-filled intradural portion of dermal sinus (*arrows*) lying posterior to conus. However, subcutaneous portion of dermal sinus (*arrowheads*) is not seen on the image with narrow windowing.**

***C–F*, Axial SE 600/20 images through conus medullaris and proximal cauda equina show fat-lined dermal sinus ascending adjacent to right posterolateral nerve roots before ending in right posterolateral aspect of conus.**

level of the conus medullaris, the location and signal characteristics of the sinus tract, and the size, location, and signal characteristics of any associated dermoid or epidermoid tumors. The MR findings were then compared with surgical findings.

Follow-up examination of patient 7 included a 3D Fourier transform gradient-echo acquisition using a volumetric RF pulse as a "spoiler" (SPGR, General Electric, Milwaukee). Sagittal 2-mm 40/5/2 images were obtained using theta = 40°.

Results

Cutaneous abnormalities were seen on the MR images in six of the seven patients. On short TR sagittal and axial images the sinus tracts and ostia were seen as linear, curvilinear, or conelike dorsal midline areas of hypointensity within the continuous layer of high-intensity subcutaneous fat (Figs. 1 and 2). The tract could sometimes be followed through the subcutaneous tissue and posterior elements of the spinal column to the dura, which was "tented" posteriorly at the site of penetration of the sac in two patients (Fig. 3). The tract coursed slightly caudally from the skin to the spine in three patients, slightly rostrally in one, and coursed straight (horizontally) in two. Proper window settings were critical in the detection of subcutaneous tracts. In patient 1, the subcutaneous tract was not seen when standard window settings were used (Fig. 1). The lack of visualization of the subcutaneous tract in patient 7 probably relates to improper windowing.

The dermal sinus tracts themselves were not visible in their intraspinal portion. Portions of the tract were detected in patient 3, in whom it was lined by fat, and in patients 1 and 7, in whom fatty material was present within a portion of the tract (Fig. 1). Aside from these three locations, the intraspinal portions of the tracts could not be detected, presumably because of their small size and their isointensity with CSF on the short TR/TE images obtained. In the patients in whom portions of the tract were visible, they ascended in the dorsal aspect of the thecal sac from their point of dural penetration to the distal spinal cord. In patient 3, the tract ascended in the midline and ended in the dorsum of the conus medullaris, whereas in patient 1, the tract ascended adjacent to the right posterior nerve roots of the cauda equina (Fig. 1) before terminating adjacent to the right posterolateral aspect of the conus. Only a small portion of the tract was seen in patient 7 (Fig. 4).

Intradural tumors were present in five patients. In three of these five the tumor was both intra- and extramedullary. Patients 2 and 4 had large (1 cm × 2½ cm) masses within the cord substance at the T8–T9 and T3–T5 levels, respectively. The masses were isointense with CSF and expanded the cord at the affected levels (Fig. 2). Extramedullary tumor components were found at surgery in both of these patients but were not detected on the images that were obtained. Patient 6 had a mass that filled the entire thecal sac from the sacrum to T12 and then extended rostrally within the cord substance from the conus (at T12–L1) to T10. The extramedullary tumor was difficult to categorize on the short TR/TE sagittal and axial images, appearing as a poorly defined iso- to slightly hyperintense mass intermingling with the roots of

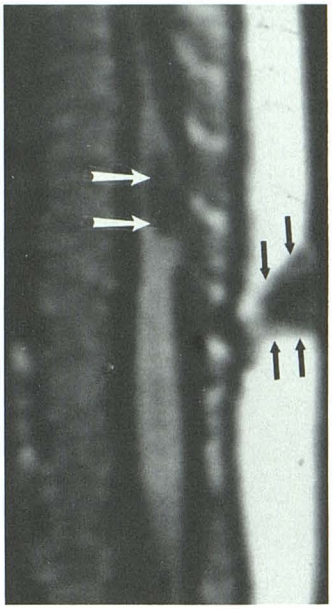

Fig. 2.—Patient 2. Sagittal SE 600/20 image shows a large cone-shaped area of hypointensity (*black arrows*) in subcutaneous fat. This is subcutaneous portion of dermal sinus. Intraspinal portion of dermal sinus is not seen. An intramedullary dermoid is seen as an oval-shaped area of hypointensity (*white arrows*) within spinal cord at T8–T9 level.

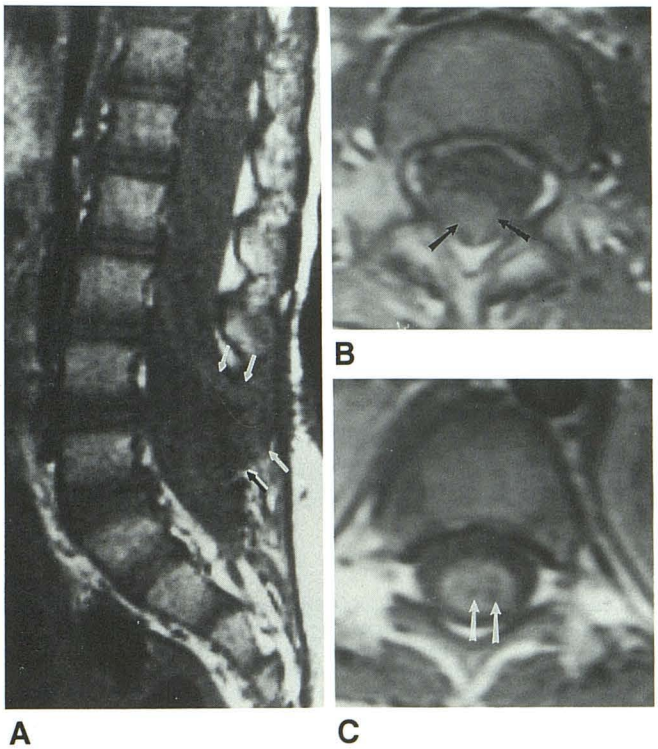

Fig. 3.—Patient 6.

***A*, Sagittal SE 1000/20 image shows spina bifida at L4 and L5 levels. Dorsal "tenting" of thecal sac (*arrows*) is present. Some streaky increased signal is present in thecal sac; this was interpreted as being misregistration artifact from abdominal motion.**

***B*, Axial SE 600/20 image at L2–L3 level shows hyperintense mass (*arrows*) filling a portion of subarachnoid space. At surgery, epidermoid tumor was seen filling entire lumbar thecal sac.**

***C*, Axial SE 1000/20 image at level of conus medullaris. Several foci of hypointensity are seen within cord substance (*arrows*). At surgery, hypointense area was found to be intramedullary epidermoid tumor.**

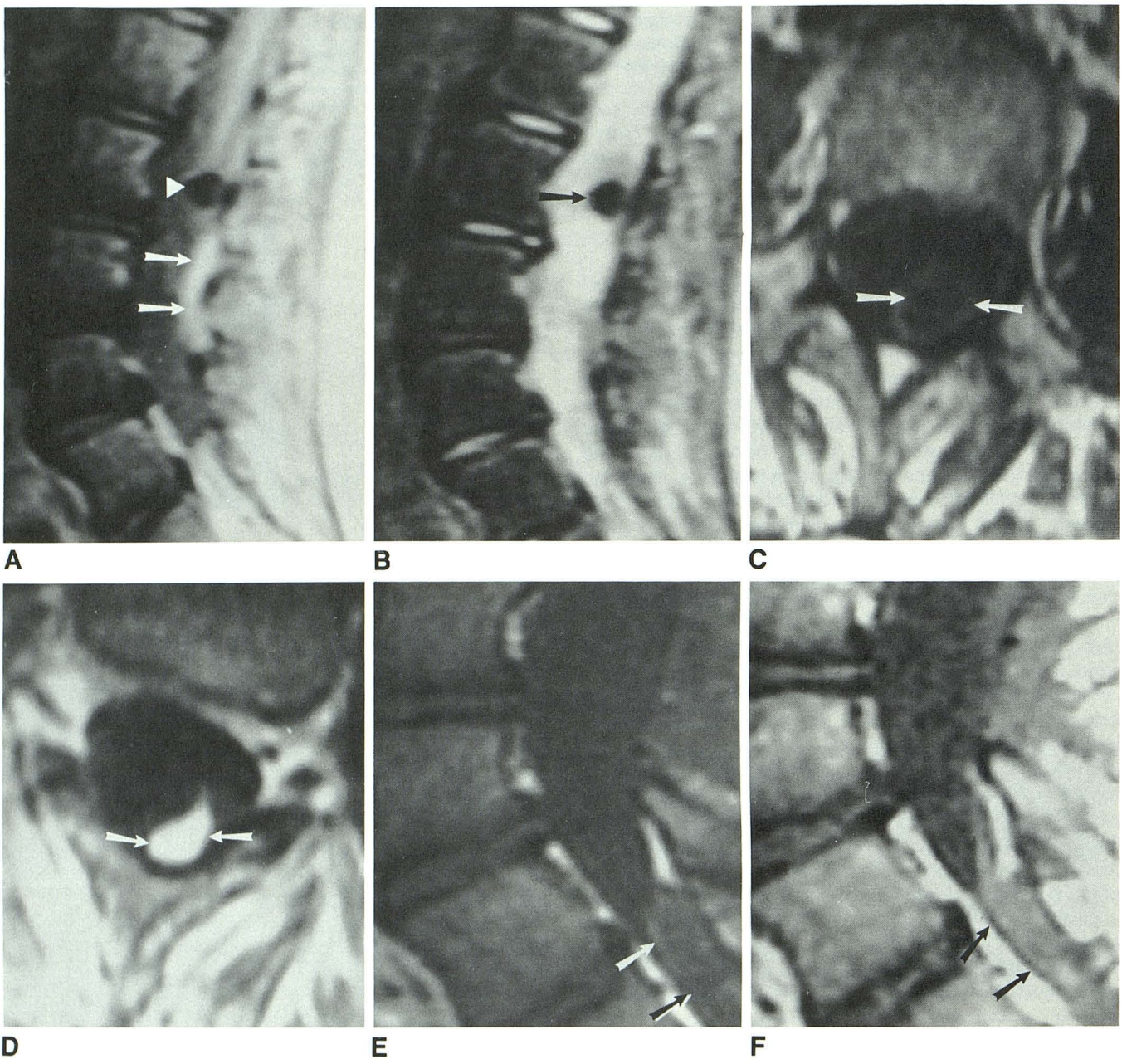

Fig. 4.—Patient 7.

A, Sagittal SE 1800/30 image shows conus medullaris ending at bottom of L2. A round area of hypointensity (*arrowhead*) is seen immediately caudal to conus. No focal lesion corresponding to this hypointensity was found at surgery. A curvilinear area of hyperintensity (*arrows*) is seen dorsally within canal at L4 level, corresponding to fat within dermal sinus tract. The remaining lumbar subarachnoid space looks normal. At surgery, the entire lumbar subarachnoid space was filled with ruptured dermoid tumor.

B, SE 1800/80 image also shows the mass at L2 (*arrow*) and a homogeneous appearance of the lumbar subarachnoid spaces.

C, Axial SE 500/20 at L3 level shows a circular positioning of nerve roots (*arrows*) within thecal sac, indicating that they are wrapped around a central mass.

D, SE 500/20 image at L4 level shows fat (*arrows*) within sinus tract in dorsal lumbar subarachnoid space.

E, SE 600/20 image 4 months after surgery. The residual dermoid tumor (*arrows*) lying in the most caudal subarachnoid space is difficult to see.

F, 3D Fourier transform gradient-echo acquisition 40/5 (theta = 40°) image provides better lesion conspicuity (*arrows*) because of the increased T1 weighting.

the cauda equina (Fig. 3). The intramedullary portion appeared as several fingerlike cords of hypointensity within the substance of the expanded spinal cord (Fig. 3). Patient 5 had an entirely extramedullary epidermoid that was found at surgery to extend from L3 to L4. The mass was invisible on sagittal spin-echo images and could only be detected on axial images by the ringlike configuration of the nerve roots of the cauda equina as they surrounded the isointense mass. Patient 7 had

a ruptured dermoid that filled the thecal sac from the sacrum to T12. Compared with extensive tumor found at surgery, the MR was minimally abnormal. Axial short TR/TE images (Fig. 4C) showed a circular arrangement of nerve roots immediately caudal to the conus, similar to what was seen in patient 4. This region was hypointense relative to neural tissue on long TR images and was initially suspected to be a focus of hemorrhage or a hemorrhagic mass. Further caudally, at the L4 and L5 levels, a curvilinear stripe of tissue with a short T1 relaxation time (described earlier) coursed through the dorsal aspect of the thecal sac (Fig. 4). The remainder of the lumbar subarachnoid space was interpreted as being normal. A follow-up scan 3 months after surgery was obtained on patient 7 using both standard spin-echo techniques and a T1-weighted 3DFT gradient-echo technique with volumetric RF spoiler (SPGR). The SPGR technique resulted in greater conspicuity of the remaining dermoid (Fig. 4F).

The conus medullaris was low-lying (and therefore presumably tethered) in four of the seven patients (Table 1). None of these had a thickened filum terminale. Although fat lined the dermal sinuses in patients 1, 3, and 7, the cord itself was not dysraphic and the lipomas did not extend all the way to the spinal cord. Therefore, the lipomas were thought to be associated lesions, not the cause of the tethering. The level of the conus in the patients with tethering ranged from L2–L3 to L4–L5.

Bone anomalies were detected by MR in three patients. Patient 3 had a spina bifida at L5 and S1, patient 5 had spina bifida of S1, and patient 6 had spina bifida of L4 and L5. Patient 7 had multilevel sacral spina bifida that was not detected by MR because the sacrum was not imaged.

Discussion

Dorsal dermal sinuses are developmental anomalies of the spine in which epithelium-lined tracts extend inward from the skin surface for a variable distance. They may terminate within the subcutaneous tissues or dura, or they may pass through the dura to terminate in the spinal cord, conus medullaris, filum terminale, a nerve root, or a fibrous nodule in the dorsal spinal cord [6]. A hyperpigmented patch, hairy nevus, or capillary angioma is usually present at the skin surface [7]. Approximately half of all dermal sinuses have associated dermoid or epidermoid cysts [8], usually at the termination of the tract. Approximately 25% of spinal dermoids are associated with dermal sinuses [6, 9, 10]. Patients typically present with infection (cutaneous abscess, intraspinal abscess, or meningitis) as a result of seeding of bacteria through the dermal sinus, or with symptoms of cord or nerve root compression by the associated dermoid or epidermoid tumor [6].

Dorsal dermal sinuses are thought to result from faulty neurulation. As has been well described [6, 11], the spinal cord forms as the result of separation of midline neural ectoderm from more lateral cutaneous ectoderm in the dorsal surface of the embryo and a nearly simultaneous closure of the neural tube. Mount [12] postulated that dorsal dermal sinuses result from focal incomplete separation of cutaneous ectoderm from neural ectoderm during the process of neurulation. When the spinal cord later becomes surrounded by mesenchyme and undergoes its relative ascent with respect to the spinal column, this adherence remains and forms a long, epithelium-lined tract (Fig. 5). Infections result from seeding of bacteria into the subcutaneous or intraspinal regions through the tract. Dermoids or epidermoids may develop as the result of desquamation of the tract lining.

Mount's proposed mechanism of formation [12] explains the phenomenon that the dermatomal level of the cutaneous defect corresponds to the neural ectodermal level of the CNS structure with which it connects via the tract (i.e., a tract with an L5 dermatomal cutaneous orifice extends to the L5 neural ectodermal level of the spinal cord). It may also explain the high rate of occurrence of tethered spinal cords in this series

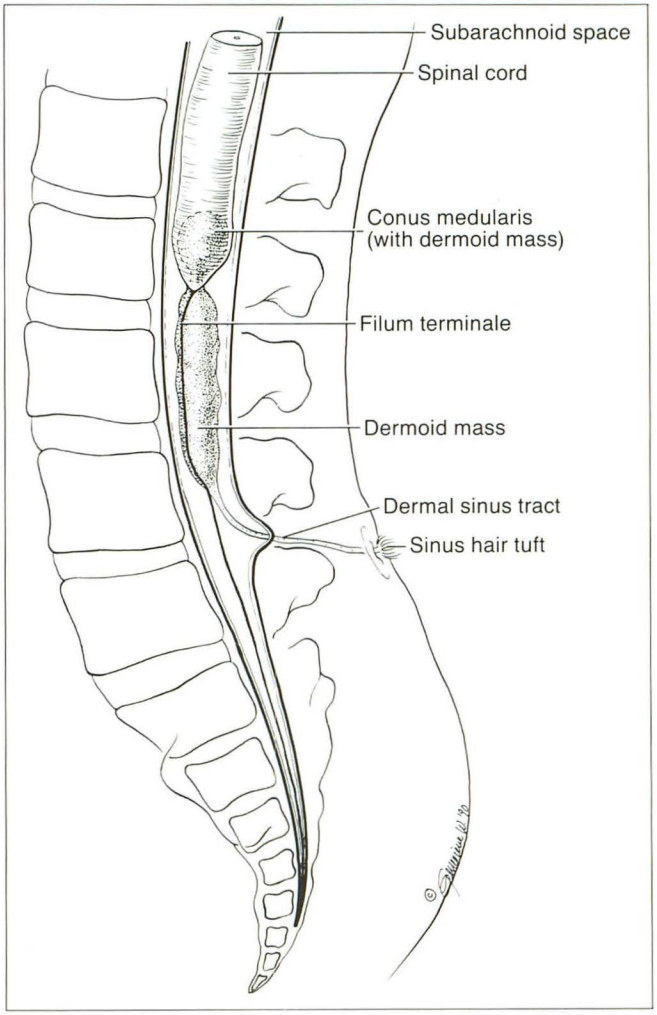

Fig. 5.—Schematic showing a typical appearance of a dorsal dermal sinus with an associated intra- and extramedullary dermoid. Epithelium-lined tract extends inward from skin surface to connect with CNS. The tract may terminate in the dura, spinal cord, conus medullaris, filum terminale, a nerve root, or a fibrous nodule in the dorsal spinal cord. A pigmented patch, hairy nevus, or capillary angioma is usually present at skin surface. Approximately half of all dermal sinuses have associated dermoid or epidermoid tumors, which are usually at the termination of the tract but may occur anywhere along the tract.

(four of seven). All of the patients with tethered cords (diagnosis made by identification of the level of the conus below the bottom of L2) had a cutaneous tract opening at L4 or below, and two of the three patients without evidence of tethering had thoracic dermal sinuses. One might, therefore, postulate that the sinus tract tethers the spinal cord in some patients. Obviously, as illustrated by patient 6, some patients with low lumbar cutaneous sinus openings have a conus positioned at the normal level.

Many of the features of dorsal dermal sinuses were seen well by standard spin-echo imaging techniques. The cutaneous and subcutaneous portions of the tracts were seen on short TR/TE images as linear, curvilinear, or conelike areas of low signal intensity coursing through the high-intensity fat (Figs. 1 and 2). Some care must be taken in the photography of these lesions, because the narrow window setting typically used for images of the spinal cord can obscure the sinus tract (Fig. 1). It is, therefore, imperative that the radiologist look at the images with variable window settings for optimal demonstration of both the intra- and extraspinal pathology. Although the cutaneous defects, cord tethering, and intramedullary tumors were demonstrated well by spin-echo MR, several critical features of the pathologic process were more difficult to identify. The intraspinal segments of the dermal sinus tracts were poorly visualized and, more importantly, diffuse subarachnoid tumor was difficult to diagnose on the basis of the MR scans in patients 6 and 7.

Adequate determination of the entire extent of the dermal sinus tract is important in preoperative planning and counseling of patients. If the tract ends external to the dura, resection is a relatively minor procedure because opening of the dura is unnecessary. If the tract extends into the thecal sac, however, the dura must be opened and the laminectomy extended rostrally, often for several levels, in order to adequately treat the patient. The tracts are composed largely of epithelial tissue (epidermis) and are, therefore, of low signal intensity on MR studies. The low signal intensity of the tract is difficult to distinguish from the low intensity of the CSF on the short TR/TE images. Moreover, the tracts are usually small in diameter and CSF pulsations almost certainly result in motion of the sinus tract within the subarachnoid space, factors that further compound the problem.

More disturbing than the lack of sensitivity in the detection of the sinus tracts is the lack of sensitivity in the detection of the extramedullary dermoid and epidermoid tumors. The appearance of CNS dermoid and epidermoid tumors on MR has been described [13–15]. Most epidermoids are nearly isointense with CSF (long T1, long T2) whereas dermoids mimic fat (short T1, short T2) on spin-echo images. However, both epidermoids with short T1 and short T2 relaxation times [16] and dermoids with long T1 and long T2 relaxation times [14, 15] have been described. In our study, all of the dermoids and epidermoids were nearly isointense with CSF on both long TR and short TR spin-echo images. Intramedullary tumors, therefore, contrasted with the adjacent spinal cord and were easily identified. However, the identification of extramedullary tumors was difficult. Although abnormalities on the MR scans of patient 6 (Fig. 3) were identified easily, determining whether the heterogeneity in the lumbar subarachnoid space represented epidermoid tumor or clumped nerve roots resulting from prior infections was not possible. Identification of the tumor in patient 7 (Fig. 4) was even more difficult. The low-lying conus medullaris and the adjacent focus of low signal intensity on long TR/short TE and long TR/long TE spin-echo images suggested tethering of the cord by a hemorrhagic mass. The surrounding subarachnoid spaces were interpreted as being normal. In retrospect, the circular pattern of the cauda equina on axial images (Fig. 4C), similar to the pattern in patient 5, and the curvilinear area of fat in the dorsal thecal sac (Figs. 4A and 4D) suggested the correct diagnosis. Nonetheless, the treating surgeon was quite surprised when, upon opening the meninges, he encountered thick, white dermoid material filling every portion of the lumbar subarachnoid space. No focal lesion was found to explain the area of short T2 relaxation time adjacent to the conus.

The lack of sensitivity of the standard spin-echo MR sequences in the detection of the intraspinal portion of the sinus tract and extramedullary tumors raises the question of the optimal way to image patients with dorsal dermal sinuses. CT myelography is excellent in the detection of the intradural portion of the sinus tract and intradural, extramedullary tumors [6] but is relatively insensitive to intramedullary processes. Sonography [17, 18] can be used in infants in the first year of life, at which time the small size of the bony posterior elements of the spinal column are small and incompletely ossified. The interlaminar spaces function as sonographic windows, allowing visualization of the sinus tract and both intra- and extramedullary tumor [17]. Unfortunately, sonography is ineffective in older children. We have noticed that SPGR images give better conspicuity of intracranial epidermoid tumors than do short TR/TE spin-echo sequences, which are considerably less T1-weighted [19]. Trying this technique in patient 7, who was known to have some residual tumor, we subjectively judged the tumor to be more easily identifiable on SPGR images. This single observation warrants further investigation of the technique in the workup of patients with dorsal dermal sinuses. It is also possible that diffusion imaging, which is helpful in the identification of intracranial epidermoids [20] may be useful in the spine. Another possibility is that T2-weighted images with motion compensation techniques (gradient moment nulling, peripheral gating) may allow more confident identification of the intraspinal portion of the sinus tract. For now, we recommend sonography or MR using heavily T1-weighted images (inversion recovery or SPGR) in infants and inversion recovery or SPGR in children more than 1 year old as the initial screening process. Plain film or CT myelography may be helpful to supplement the information obtained by the less invasive methods, although in patients 6 and 7 lumbar puncture would have been unsuccessful and myelography would certainly have shown a myelographic block at approximately T12 after subsequent cervical puncture. The surgeon, therefore, would nevertheless have been unaware of what he was going to find at laminectomy.

To summarize, a review of the MR and surgical findings in seven patients with dorsal dermal sinuses revealed that stand-

ard spin-echo imaging techniques are excellent for the detection of the subcutaneous portion of the sinus tract, intermedullary dermoid or epidermoid tumor, and associated cord tethering. However, the intraspinal segment of the sinus tract and extramedullary tumor were very difficult to identify. Optimal radiologic workup of patients with dorsal dermal sinuses awaits the development of new MR imaging sequences. For now, heavily T1-weighted MR sequences should be obtained and supplemented with sonography in infants and with CT myelography in children more than 1 year old.

REFERENCES

1. Barkovich AJ. *Pediatric neuroimaging*. New York: Raven Press, **1990**
2. Barkovich AJ, Chuang SH, Norman D. Anomalies of neuronal migration: MRI. *AJNR* **1987**;8:1009–1017
3. Smith AS, Weinstein MA, Quencer RM, et al. Association of heterotopic gray matter with seizures: MR imaging. *Radiology* **1988**;168:195–198
4. Davis PC, Hoffman JC Jr, Ball TI, et al. Spinal abnormalities in pediatric patients: MR imaging findings compared with clinical, myelographic, and surgical findings. *Radiology* **1988**;166:679–685
5. Raghavan N, Barkovich AJ, Edwards MSB, Norman D. MR imaging in the tethered cord syndrome. *AJNR* **1989**;10:27–36
6. Naidich TP, McLone DG, Harwood-Nash DC. Spinal dysraphism. In: Newton TH, Potts DG, eds. *Modern neuroradiology*, vol. 1. *Computed tomography of the spine and spinal cord*. San Anselmo, CA: Clavadel Press, **1982**: 299–353
7. Haworth JC, Zachary RB. Congenital dermal sinuses in children: their relation to pilonidal sinuses. *Lancet* **1955**;2:10–14
8. Cardell BS, Laurance B. Congenital dermal sinuses associated with meningitis: report of a fatal case. *Br Med J* **1951**;2:1558–1561
9. Harwood-Nash DC, Fitz CR. *Neuroradiology in infants and children*, Vol. 3. St. Louis: Mosby, **1976**: 1054–1227
10. Guidetti B, Gagliardi FM. Epidermoid and dermoid cysts: clinical evaluation and late surgical results. *J Neurosurg* **1977**;47:12–18
11. Naidich TP, McLone D. Growth and development. In: Kricun ME, ed. *Imaging modalities in spinal disorders*. Philadelphia: Saunders, **1988**: 1–19
12. Mount LA. Congenital dermal sinuses as a cause of meningitis, intraspinal abscess, and intracranial abscess. *JAMA* **1949**;139:1263–1268
13. Vion-Dury J, Vincentelli F, Jiddane M, et al. MR imaging of epidermoid cysts. *Neuroradiology* **1987**;29:333–338
14. Newton DR, Larson TC, Dillon WP, Newton TH. Magnetic resonance characteristics of cranial epidermoid and teratomatous tumors. *AJNR* **1987**;8:945
15. Awwad EE, Backer R, Archer CR. The imaging of an intraspinal cervical dermoid tumor by MR, CT, and sonography. *Comput Radiol* **1987**;11: 169–173
16. Horowitz BL, Chari MV, James R, Bryan RN. MR of intracranial epidermoid tumors: correlation of in vivo imaging with in vitro C-13 spectroscopy. *AJNR* **1990**;11:299–302
17. Kangarloo H, Gold RH, Diament MJ, Boechat MI, Barrett C. High-resolution spinal sonography in infants. *AJNR* **1984**;5:191–195
18. Naidich TP, Gorey M, Raybaud C, McLone DG, Byrd SE. Malformations congenitales de la moelle. In: Manelfe C, ed. *Imagerie du rachis et de la moelle*. Paris: Vigot, **1988**:571–620
19. Crawley AP, Wood ML, Henkelman RM. Elimination of transverse coherences in FLASH MRI. *Magn Reson Med* **1988**;8:248–260
20. Tsuruda JS, Chew WM, Moseley ME, Norman D. Diffusion-weighted MR imaging of the brain: value of differentiating between extraaxial cysts and epidermoid tumors. *AJNR* **1990**;11:925–931